ANALYSIS OF DEFECTS AND DAMAGE IN COMPOSITES

G. C. Sih

Institute of Fracture and Solid Mechanics, Lehigh University, Bethlehem, PA 18015, USA

ABSTRACT

Preexisting defects and damage under load introduce additional inhomogeneities that make analytical modeling of composite systems difficult. The non-homogeneous and/or anisotropic character of composite behavior is load time history dependent and invalidates many of the testing procedures developed for the more traditional monolithic materials. Composite specimens even though are simplified in terms of loading and geometric configuration respond inherently as structures. The relative response between any two composite systems is case-specific and has to be validated through analysis and experiment.

This communication addresses a number of topics that require scrutiny in the prediction of composite material behavior and/or failure. The dominant flaw model can yield useful information in situations where subcritical material damage has a negligible influence on the energy released at incipient fracture. Analytical modeling of interface behavior between fiber and matrix or laminae is not always straightforward because load transmission from one material to another is affected by stress state in addition to being material dependent. Emphasized is the quantitative assessment of the degree of local inhomogeneity which can be measured by fluctuation of the strain energy density function, dW/dV. The local and global stationary values of dW/dV are found not only useful for identifying the sites of possible failure and yielding but also the stability of composite systems that depends on the combination of loading, geometry and material inhomogeneity.

Composites being vulnerable to aggressive environmental changes can behave very differently when the moisture and temperature conditions are altered. Results are presented for a crack in T300/5208 graphite fiber laminate subjected to moisture, temperature and stress boundary conditions. These influences can, in general, be coupled and lead to failure modes that are not intuitively obvious.

KEYWORDS

Composite materials, fibers, epoxy resin, defects, cracks, interface, fracture toughness, inhomogeneity, anisotropy, laminate, moisture, temperature, coupling, strain energy density, stationary values, system instability.

INTRODUCTION

Over the past two decades, composites have gained wide acceptance as construction materials and load supporting members in both commercial and military applications. An unique advantage of the multicomponent material systems lies in the added flexibility in design such that the mechanical, thermal and electrical properties can be tailor-made to simultaneously match multifaceted requirements. This is usually accomplished by embedding fibers in resins and adjusting the volume fractions of the constituents and their arrangements until the desired combination is obtained. Subcomponents such as unidirectionally reinforced elements are first made and stacked in sequence to form a laminate structure. Hybrid systems involving two or more families of reinforcing fibers are also becoming more common. The degree of freedom gained in composite system design, however, is not altogether penalty free. Inhomogeneity and anisotropy of the internal structure are more readily reflected through composite materials as compared with the traditional monolithic materials. Defects and material damage in the form of fiber breaking, matrix cracking and delamination are considered desirable from the viewpoint of reducing the available energy to cause catastrophic fracture. The complexities of subcritical local failure do introduce additional uncertainties into the analysis, particularly when size of the defects or irregularities are comparable with the dimensions of the internal structuring. Loading type and sequence can also seriously affect the rate at which defects are created and grow. This load time history dependent process of material damage controls the performance of composites, the quantitative assessment of which is most lacking.

Despite the extensive research efforts in the past (Sih and Tamuzh, 1978; Sih and Tamuzh, 1981), the understanding of composite material behavior lags far behind its need in application. Progress has directed mostly towards improving manufacturing techniques and strength of specimens tested under simple laboratory conditions. It has now become increasingly apparent that the mere application of nonhomogeneous and/or anisotropic continuum theories is hardly sufficient. Instead of emphasizing computational methods, attention should be focused on establishing a rational approach supported by theory. Failure concepts and specimen testing procedures developed for homogeneous materials are not applicable to composites in general. The translation of uniaxial test data to multiaxial stress states rely on *homogeneity* in stress field and material property and becomes questionable when inhomogeneity is present. Stress state in composite specimens is inherently complex even when loading is uniaxial. The internal physical structure of composites is scaled such that their behavior is extremely sensitive to load orientation. A case in point is the fracture toughness[1] testing of composite specimens. Material damage in multicomponent systems will not be dominated by the energy release of a single crack. The creation of free surface in fibers relative to the matrix dissipates energy and is load direction dependent. The failure to account for fiber and matrix breaking in fracture

[1]Fracture toughness (Sih, 1976) originally developed to characterize metal alloys applies strictly to a homogeneous body whose uniaxial test properties can be used to calculate the energy released for creating a unit area of free surface at the onset of rapid fracture.

toughness testing and calculation results in little useful information because the critical load would then serve the same purpose.

As in all disciplines of science and technology, there exists not a general solution to all specific situations. Strictly speaking, all materials are composites because the mechanical properties of their constituents are different. The grains in a polycrystalline metal alloy differ from one location to another at the microscopic level. Their behavior, when characterized under monotonic loading, can be adequately described through the macroscopic parameters such as yield strength, fracture toughness, etc., upon invoking the assumption of homogeneity. Microstructure effects, however, can no longer be ignored when the loading becomes cyclic or is sustained on the specimen for a long period of time as in creep. It is, therefore, the interaction of loading with material microstructure that controls the damage and hence the degree of homogeneity or inhomogeneity in a system. This communication shall concentrate on several essential features of composite material behavior that are in need of clarification and further advancement. These areas may be outlined briefly as follows:

(1) Dominant flaw model

(2) Interface behavior in multicomponent system

(3) Assessment of material inhomogeneity

(4) Interdependence of moisture, temperature and stress

Analytical modeling of composite behavior has been problematic as it involves the selection of material damage criteria. There is the widespread tendency to empirically match analytical results with experimental data. The agreements are short lived as the operational conditions are changed. It is not uncommon to find several criteria[2] in explaining a single physical phenomenon. The lack of *consistency* in analysis explains why little progress has been made in the failure prediction of composite materials in the past decade (Sih et al, 1973).

DOMINANT FLAW MODEL

Linear elastic fracture mechanics (LEFM) is the simplest material damage model that addresses sudden global fracture initiating from a dominant flaw or crack[3] although the body may contain a number of preexisting flaws. This is partly because the discipline does not treat subcritical crack growth. Such an ideal situation can model those composite systems that fail suddenly from an initial flaw or imperfection with negligible amount of subcritical damage. Experiments have shown that the onset of brittle fracture can indeed initiate from a single dominant defect or crack in fiber-glass reinforced plastics (Wu and Reuter, 1965), (Lauraitis, 1971) and (Lauraitis, 1971) and graphite epoxy composites (Sih et al, 1975).

[2]The von Mises' yield criterion is usually applied to determine the extent of plastic flow while a separate condition such as maximum strain, crack opening displacement or other parameter is invoked for crack growth.

[3]It is theoretically possible to pose an ideal situation where the onset of rapid fracture initiates from the tips of two separate cracks. Such a condition should be excluded from reality due to the absence of perfect symmetry and load alignment.

Scotchply 1002: Unidirectional Specimens

As mentioned earlier, the dominant flaw model concerns with the sudden release of energy in a unit volume of material that triggers global instability. This concept will be applied to analyze the failure of Scotchply 1002, a trade name by the Minnesota Mining and Manufacturing Company. It is a unidirectional composite with transverse isotropy in the 2-3 plane. With reference to Fig. 1(a), the 1- and 2-direction correspond, respectively, to

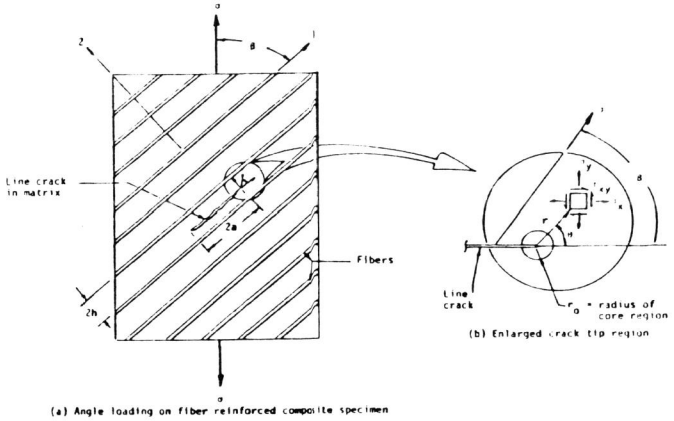

Fig. 1. Matrix crack in unidirectional fiber reinforced composite under angle loading.

the longitudinal and transverse fiber direction while the 3-direction being normal to the 1-2 plane is not shown. The orthotropic elastic constants may be obtained from (Sih and Chen, 1973)

$$E_1 = E_{f_1}V_f + E_mV_m,\quad E_2 = \left[\frac{E_{f_2}+E_m+(E_{f_2}-E_m)V_f}{E_{f_2}+E_m-(E_{f_2}-E_m)V_f}\right]E_m$$

$$\nu_{12} = \nu_fV_f + \nu_mV_m,\quad \nu_{23} = \nu_fV_f + \left[\frac{1+\nu_m-\nu_{12}E_m/E_1}{1-\nu_m^2+\nu_m\nu_{12}E_m/E_1}\right]\nu \qquad (1)$$

$$\mu_{12} = \left[\frac{\mu_f+\mu_m+(\mu_f-\mu_m)V_f}{\mu_f+\mu_m-(\mu_f-\mu_m)V_f}\right]\mu_m$$

The definitions of the various constants in Eq. (1) are as follows:

E_{f_1} = fiber longitudinal Young's modulus,

E_{f_2} = fiber transverse Young's modulus,

V_f = fiber volume fraction,

V_m = matrix volume fraction,

μ_f = fiber shear modulus,

μ_m = matrix shear modulus,

ν_f = fiber Poisson's ratio, (2)

ν_m = matrix Poisson's ratio

The epoxy resin is isotropic and hence the matrix Young's modulus E_m is related to μ_m by $E_m = 2\mu_m(1+\nu_m)$. For a 56.5% fiber volume fraction, E_m = 3.10 MPa and ν_m = 0.35, the properties of the glass fibers may be substituted into Eqs. (1) to yield

$$E_1 = 34.47\ \text{MPa},\ \nu_{12} = 0.05$$

$$E_2 = 11.51\ \text{MPa},\ \mu_{12} = 4.85\ \text{MPa} \qquad (3)$$

A defect or crack of length 2a is assumed to exist in the epoxy resin, Fig. 1(a). The fiber spacing 2h for V_f = 0.565 is very small in comparison with 2(a). This permits an asymptotic evaluation of the crack tip stress intensity that will be given subsequently.

Failure Analysis

As the applied load σ in Fig. 1(a) is directed at an angle β with reference to the crack plane, the elastic crack tip stress field[4] involves both k_1 and k_2 (Hilton and Sih, 1972):

$$k_1 = \Phi(1)\sigma\sqrt{a}\,\sin\beta,\quad k_2 = \Psi(1)\sigma\sqrt{a}\,\sin\beta\cos\beta \qquad (4)$$

in which $\Phi(1)$ and $\Psi(1)$ for Scotchply 1002 are found to be

$$\Phi(1) = 0.290,\quad \Psi(1) = 0.170 \qquad (5)$$

for the case $h/a \ll 1$. In view of Eqs. (4), failure initiation will be governed by the combination of k_1 and k_2 and the crack will not extend collinearly[5]. This invalidates the usage of the classical energy release rate approach that relies on self-similar crack growth. Reference is thus made to the strain energy density criterion (Sih, 1973; and Sih, 1981) which has been used extensively for analyzing the influence of defects or cracks on composite material behavior (Sih and Chen, 1981).

The state of affairs in the immediate vicinity of the crack tip is excluded from the analysis by the appropriate selection of a core region with radius

[4]Refer also to the Appendix (Sih and Chen, 1973) for the evaluation of k_1 and k_2.

[5]The matrix crack will initiate noncollinearly although crack propagation may continue along the fiber after initiation. Remember that onset of rapid fracture concerns with only the instant at which energy is released suddenly to extend a very small segment of the crack. What occurs therefore after is beyond the scope of the analysis.

r_o, Fig. 1(b). Failure is assumed to coincide with the strain energy density function dW/dV in element with stress components σ_x, σ_y and τ_{xy} reaching a critical value[6] $(dW/dV)_c$. Since global instability is assumed to be initiated by cracking in the epoxy resin, only a knowledge of $(dW/dV)_c$ for the matrix material is necessary. Without loss in generality, a strain energy density factor S may be defined:

$$\frac{dW}{dV} = \frac{S}{r} \tag{6}$$

If r is taken as a fixed distance from the crack tip the element that triggers fracture, it then suffices to consider[7] (Sih, 1973; and Sih, 1981)

$$S = a_{11}k_1^2 + 2a_{12}k_1k_2 + a_{22}k_2^2 \tag{7}$$

The coefficients a_{ij} are functions of elastic constants and θ as defined in Fig. 1(b). According to the strain energy density criterion, the direction of crack initiation may be determined by taking $\partial S/\partial\theta = 0$ and finding $\theta = \theta_o$ for which S is a local minimum. The condition of fracture coincides with $S = S_c$. This yields an expression

$$S_c = \sigma_c^2 a F(\beta,\theta_o) \tag{8}$$

The function $F(\beta,\theta_o)$ gives θ_o through a_{ij} (i,j = 1,2) as given by

$$F(\beta,\theta_o) = 0.084\, a_{11}\sin^4\beta + 0.049\, a_{12}\sin^3\beta\cos\beta + 0.029\, a_{22}\cos^4\beta \tag{9}$$

For each β, a corresponding angle of fracture θ_o can be calculated from Eq. (9). An approximate value of $\theta_o \simeq 55°$ is found for $\beta = 30°$ which exhibits the influence of material inhomogeneity on crack growth direction.

Knowing[8] $S_c = 9.63$ N/m for the epoxy resin, Eq. (8) may be evaluated numerically for σ_c, a and β. The results are compared to test data obtained from

[6]The quantity $(dW/dV)_c$ is the area under the true stress and strain curve at fracture. For a linear elastic material, it can be computed from $\sigma_u^2/2E$ where σ_u is the ultimate stress. For nonlinear materials, $dW/dV = \int_o^{\varepsilon_{ij}} \sigma_{ij}d\varepsilon_{ij}$ with σ_{ij} and ε_{ij} being the stress and strain components.

[7]For nonlinear materials, S can no longer be expressed in terms of the stress intensity factors and must be reevaluated depending on the constitutive equations under consideration.

[8]S_c is related to K_{1c} by the formula

$$S_c = \frac{(1+\nu)(1-2\nu)K_{1c}^2}{2\pi E}$$

where $K_1 = k_1\sqrt{\pi}$. Hence, the standard ASTM method (Brown and Srawley, 1966) applies also to the evaluation of S_c.

precracked (Wu and Reuter, 1965) and uncracked (Lauraitis, 1971) unidirectional Scotchply 1002 fiber composites in steel form. The specimens (Wu and Reuter, 1965) contain central cracks in the matrix along the fiber direction. The solid curves in Fig. 2 show the variation of the critical stress

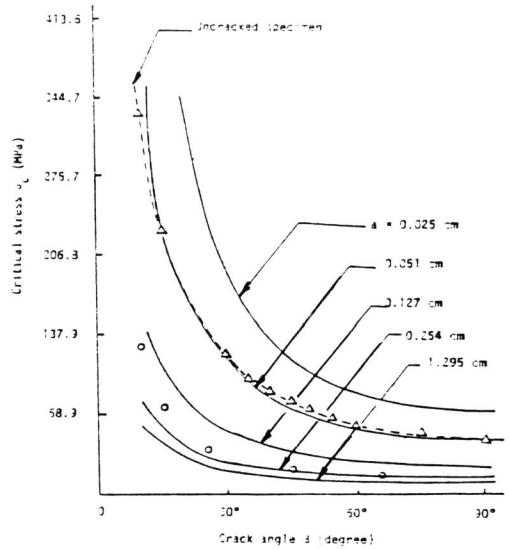

Fig. 2. Variations of critical stress with crack angle for cracked and uncracked Scotchply 1002 specimens.

σ_c with the crack angle β for five different half crack length a = 0.025, 0.051, 0.127, 0.254 and 1.295 cm. The open circles are the experimental data (Wu and Reuter, 1965) for $a \simeq 0.254$ cm. Note that they agree well with theory for large β and tend to deviate substantially as β is decreased. This is because the analytical model considered only matrix cracking and neglected fiber damage which becomes important for small β. The dotted curve pertains to the uncracked specimen data (Lauraitis, 1971) and match closely with the theoretical prediction for $a \simeq 0.051$ cm. This suggests that even though the specimens were not precracked, brittle fracture initiated from small defects in the epoxy resin. Indeed, microscopic examinations (Lauraitis, 1971) revealed that small defects of the same size existed in the material due to poor bonding and air-bubbles trapped in the matrix.

A plot of σ_c versus a for β = 10°, 15°, 25°, 45° and 90° is displayed in Fig. 3. The open circles are taken from the data (Wu and Reuter, 1965). The good agreement between theory and experiment is more clearly exhibited for β = 45° and 90° when the fibers are almost normal to the applied load. Deviations increase when β is decreased as explained earlier.

Angle-Ply Laminate

The failure modes in angle-ply laminates are considerably more complex as they may involve delamination in addition to those that occur in unidirec-

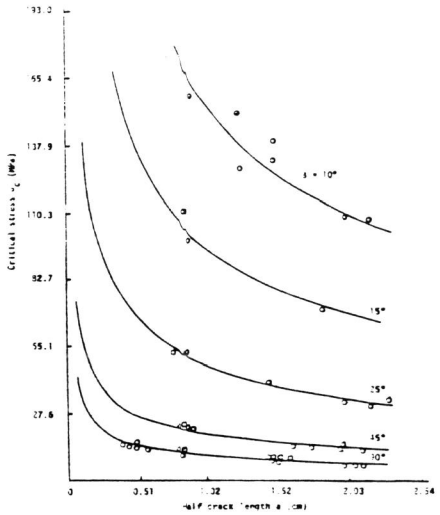

Fig. 3. Variations of critical stress with half crack length in Scotchply 1002.

tional fiber reinforced composites. Test results (Lauraitis, 1971) showed that glass fiber laminates can fail by a combination of thru-lamina and interlaminar (or delamination) cracking. These two modes tend to trade off with one another as the ply-angle[9] is varied. Sih and Chen (1973) modeled the laminate (Lauraitis, 1971) as a four-layered composite plate with perfect bonding between the laminae with no loss in load transfer. This implies that delamination[10] should be kept to a minimum with thru-lamina cracking being the dominant mode of failure as observed by Lauraitis (1971) for $45° \leq |\beta| \leq 90°$. This laminate is also assumed to have lost its structure integrity when one of the laminae has undergone rapid crack propagation.

Based on the aforementioned assumptions, the stress and failure analysis are similar to those for the unidirectional case. Adjustment is made only on k_1 and k_2 as the load transfer to a through crack in a laminate is now different. The results are shown in Fig. 4 which plots σ_c as a function of $\pm\beta$. The five data points corresponding to $\beta = \pm 15°, \pm 30°, \pm 45°, \pm 60°$ and $\pm 75°$ are those obtained by Lauraitis (1971) for a four-layered Scotchply laminate specimen 25.40 cm long and 0.127 cm thick. The thickness of each ply is approximately 0.0254 cm not counting for the adhesive layers. With half crack length $a \simeq 0.076$ cm, the theoretical prediction is good for $\beta \geq 30°$.

[9] The ply-angle coincides with the orientation of the load with the fibers, Fig. 4.

[10] The free edges on laboratory specimens tend to enhance delamination which may not be realistic for structural components that are enclosed.

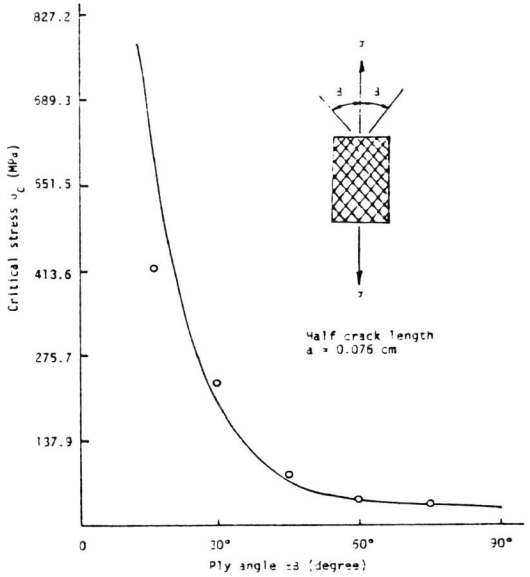

Fig. 4. Critical stress versus ply angle for Scotchply 1002 fiberglass.

INTERFACE BEHAVIOR

It is now well-known that chemical treatment of fibers can greatly influence the transfer of load across the interface of fibers and matrix and hence the gross behavior of the composite system. A fundamental drawback of any analysis lies in not knowing the mechanical properties of the interface layer. The standard approach is to assume a zero thickness dividing line between two adjoining materials and continuity of the displacement and stress field. The material properties across the interface, therefore, take a discontinuous jump from those of the fiber to those of the matrix or from one layer to another in the case of a laminate. Such a condition, of course, is unattainable in reality. There must necessarily be a finite thickness interface layer within which the material properties change more gradually. Modelling of the interface as a sum of many sublayers[11] of finite thickness results in a smoother transition. The dilemma is that interface properties are by the definition, not measurable and yet they control the load transmission characteristics which are stress and/or displacement boundary condition dependent. The philosophy adopted here is to determine those situations where the exact variations of the material properties within the interface will not appreciably influence the gross behavior of the composite. In this way, the interface may be easily modelled by the average properties upon which reliable analytical predictions could be made. Designers should avoid those combinations of loading, geometry and material type where the composite behavior is sensitive to conditions at the interface.

[11] Although additional interfaces are introduced for each sublayer across which the bondings are assumed to be perfect, the errors are suppressed to a lower scale level. The accuracy of any analysis stops short at a limiting distance which in the continuum theory is microscopic in size.

Influence of Analytical Modeling

To illustrate the idea of this approach, four different loadings for an interface between glass and epoxy I and graphite and epoxy II are considered as shown in Fig. 5.

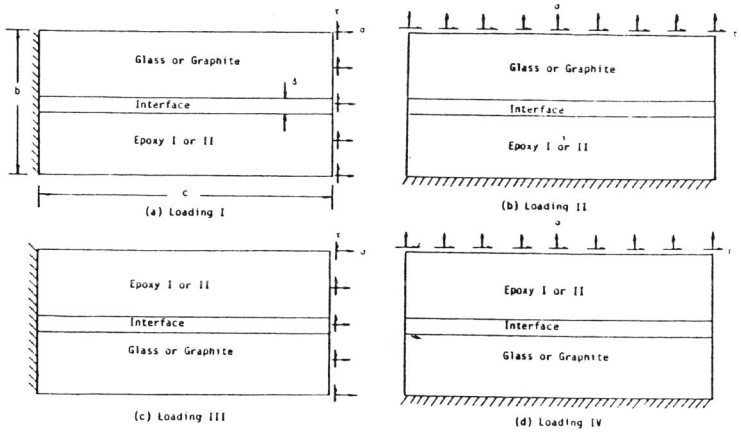

Fig. 5. Four loading cases for dissimilar material system with finite thickness interface.

The composite systems in Fig. 5 are such that c = 2b and the interface thickness δ = 0.05b. Both the applied normal stress σ and shear stress τ are set at 10^5 Pa while ν is kept at a constant value of 0.3 for all materials including that for the interface. Only the effect of variation in the Young's modulus E is studied. The data (Sih et al, 1975) on E for the glass, graphite and two different epoxy materials will be used and are given in Table 1. The two composite systems are glass-epoxy I as one combination and

TABLE 1 Young's Modulus for Different Materials

Material	E (x 10^9 Pa)
Glass	72.4
Graphite	345.0
Epoxy I	3.10
Epoxy II	3.45

graphite-epoxy II as the other. As stated earlier, the interface is divided into several finite layers[12] with a varying modulus. Analyzed are four models for each material combination (Fig. 6). For both cases, Model I in Fig. 6(a) assumes a linear modulus variation with an average modulus of E_{ave} equal to the average of that for the adjoining materials. A less gradual variation

[12]This is done in the finite element analysis such that a varying modulus across the interface can be accommodated.

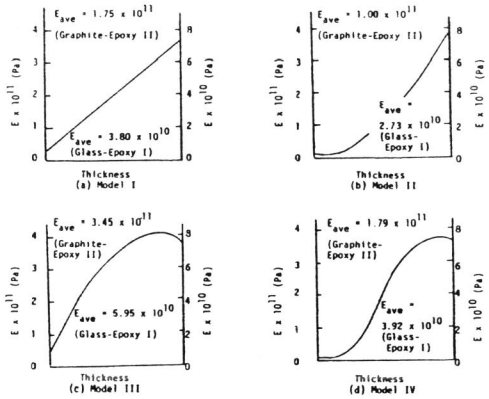

Fig. 6. Interface models for glass-epoxy I and graphite-epoxy II material combination.

of E is depicted in Fig. 6(b) for Model II. This yields a softer average modulus than Model I. Model III in Fig. 6(c) has a stiffer average modulus than Model I and a sharper initial rise in E. The variation of E for Model IV pertains to that shown in Fig. 6(d). The convexity of the curve changes while the average modulus is nearly the same as that of Model I.

In order to demonstrate how interface modeling affects the failure of composites, it is necessary to establish a theoretical basis for making predictions. Since the strain energy density criterion applies to bodies with or without initial cracks[13], it will be employed to investigate the possible failure sites of the composite systems in Figs. 5. This requires the calculation of dW/dV in plane strain.

$$\frac{dW}{dV} = \frac{1-\nu^2}{2E}(\sigma_1^2+\sigma_2^2) - \frac{\nu(1+\nu)}{E}\sigma_1\sigma_2 \qquad (10)$$

where σ_1 and σ_2 are the principal stresses in the glass or graphite. Failure is assumed to occur when the maximum of the minimum dW/dV or $(dW/dV)^{max}_{min}$ reaches the critical value $(dW/dV)_c$. Although failure would most likely first occur in the epoxy, only the $(dW/dV)_{min}$ values in the glass and graphite will be reported. This is because the finite element grid sizes are not sufficiently refined to determine the minima of dW/dV in the epoxy since its modulus of elasticity is many times lower than that of the glass or graphite. The values of $(dW/dV)^{max}_{min}$ in Table 2, however, suffice to illustrate the influence of interface modeling on failure prediction. Constant (dW/dV) con-

[13]The classical fracture mechanics concept applies only to systems with preexisting cracks.

TABLE 2 Maximum $(dW/dV)_{min}$ for Glass-Epoxy I and Graphite-Epoxy II Systems

Loading Type	Model Type	$(dW/dV)^{max}_{min}$ (J/m³) Glass-Epoxy I	Graphite-Epoxy II
I	I	4.67×10^{-1}	1.08
	II	5.47×10^{-1}	1.24
	III	4.64×10^{-1}	1.05
	IV	5.51×10^{-1}	1.29
II	I	4.74	4.77
	II	4.62	4.68
	III	4.71	4.76
	IV	4.57	4.69
III	I	2.76×10^{-1}	4.66×10^{-2}
	IV	2.11×10^{-1}	4.88×10^{-2}
IV	I	5.07×10^{-2}	1.05×10^{-2}
	IV	5.99×10^{-2}	1.08×10^{-2}

tours are obtained to determine the magnitude and location of $(dW/dV)^{max}_{min}$. Referring to Table 2, the largest values $(dW/dV)_{min}$ = 4.74 for the glass and 4.77 for the graphite corresponded to the interface Model I and Loading II while the smallest values $(dW/dV)_{min} = 5.07 \times 10^{-2}$ for the glass and 1.05×10^{-2} for the graphite corresponded to Model I and Loading IV. It would appear that Loading II is more severe than the other loading cases. For both composites tested with Loading I, the relative intensity of $(dW/dV)^{max}_{min}$ is lower for interface Models I and III than for Models II and IV. Stiffening of the interface has the effect of delaying the onset of failure in this loading case. In general, the interface modeling is shown to have a large influence on $(dW/dV)_{min}$ and is particularly sensitive to loading type. The orders of magnitude difference in $(dW/dV)^{max}_{min}$ shown in Table 2 exhibits this effect. Combination of materials also reacts with loading. Refer to the work of Sih and Moyer (1979) for more details.

Cohesive and Adhesive Failure

Failure initiating from defects near the interface can occur in two ways that may be distinguished as cohesive and adhesive failure shown in Figs. 7(a) and 7(b). Cohesive failure refers to an imperfect bond modelled as a crack and an element of material is assumed to break off to the side in the epoxy with elastic properties μ_p and ν_p. The properties of the adjoining metal are denoted by μ_m and ν_m. Figure 7(b) models adhesive failure with a crack in the epoxy away from the interface. The critical stress σ_c corresponding to crack extension will invariably be failure mode dependent.

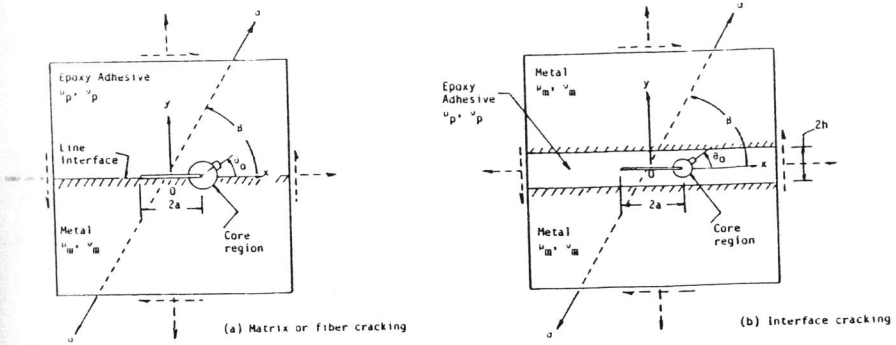

Fig. 7. Cohesive and adhesive failure.

When a crack is located at the interface of two dissimilar materials, both stress intensity factors k_1 and k_2 prevail even if the load is applied symmetrically with reference to the crack with $\beta = 90°$ in Fig. 7(a). Rice and Sih (1965) have shown that

$$k_1 = \frac{\sigma\sqrt{a}\,[\cos(\varepsilon\log 2a)+2\varepsilon\sin(\varepsilon\log 2a)]}{\cosh(\pi\varepsilon)}$$

$$k_2 = -\frac{\sigma\sqrt{a}\,[\sin(\varepsilon\log 2a)-2\varepsilon\cos(\varepsilon\log 2a)]}{\cosh(\pi\varepsilon)} \qquad (11)$$

The bi-elastic constant ε is given by

$$\varepsilon = \frac{1}{2\pi}\log\left[\frac{\kappa_p/\mu_p+1/\mu_m}{\kappa_p/\mu_m+1/\mu_p}\right] \qquad (12)$$

in which $\kappa_p = 3-4\nu_p$. The material properties of the epoxy and metal are listed in Table 3. Let r be fixed at 0.005a and it suffices to consider S in the strain energy density theory which takes the same form as Eq. (7) except that the coefficients a_{ij} (i,j = 1,2) depend on the elastic constants ν_p, ν_p and μ_m, ν_m in Table 3. They have been obtained by Sih (1973). By

TABLE 3 Elastic Constants of Epoxy and Metal

Material Type	Poisson's Ratio	Young's Modulus (MPa)	Shear Modulus (MPa)
Epoxy	0.35	3.10	1.15
Metal	0.22	68.95	28.27

taking the derivative of S with respect to θ and setting the result to zero, the directions of crack initiation are found for five different half crack length a = 0.25, 0.51, 0.76, 1.02 and 1.27 cm. The critical cohesive fail-

ure stress σ_c is then found by letting $S_{min} = S_c = 9.63$ N/m for the epoxy. The results are given in Table 4 and displayed graphically in Fig. 8. It is seen that σ_c decreases monotonically with the half crack length a.

TABLE 4 Cohesive Failure Stress for Epoxy to Metal Joint

Half Crack Length a (cm)	Fracture Angle θ_o (degree)	Normalized Stress Energy Density Factor $16\mu_p S_{min}/\sigma^2 a$	Critical Stress σ_c (MPa)
0.25	11.18°	0.939	8.62
0.51	14.85°	0.949	6.07
0.76	17.00°	0.950	4.95
1.02	18.52°	0.955	4.27
1.27	19.69°	0.958	3.81

The critical adhesive failure stress σ_c may be obtained by first calculating S_{min} for a cracked epoxy layer between two metals as illustrated in Fig. 9:

$$S_{min} = a_{11}k_1^2 = \frac{4(1-2\nu_p)}{16\mu_p}\,\phi^2(1)\sigma^2 a \qquad (13)$$

in which $\phi(1)$ depends on h/a. The final results for h/a = 0.1, 0.5 and 1.0 are given in Fig. 9 for σ applied normal to the adhesive joint. If a = 0.25 cm, Fig. 9 yields a critical adhesive failure stress of $\sigma_c = 27.89$ MPa which is considerably higher than the cohesive failure stress $\sigma_c = 8.62$ MPa for the same crack size. This conclusion indicates that imperfect bonding is much more damaging than defects in the adhesive layer. The curves in Fig. 9 also show that adhesive failure stresses are sensitive to h/a ratio for small defects.

MATERIAL INHOMOGENEITY

The interaction of load and material inhomogeneity controls failure. Sih (1984) has discussed this effect in conjunction with the initiation of failure in polycrystalline metals under fatigue. The progressive deterioration of a material element in fatigue can be attributed to the cyclic accumulation of microdistortion in the weaker crystals which are surrounded by the stronger grains behaving elastically as a whole. The nonhomogeneity from grain to grain causes a fluctuation of energy in each unit volume of material, the magnitude of which is load time dependent. The amplitude and frequency of this fluctuation can be used as a measure of *homogeneity*, a condition that must be satisfied in the standardizing of material properties through testing. Quantities such as yield strength and fracture toughness are measured under conditions where the load distribution and material microstructure are both sufficiently smooth and homogeneous at the macroscopic level. This, of course, does not apply to fiber reinforced composites that are highly inhomogeneous and their overall properties collected from uniaxial tests cannot be used reliably to predict the behavior of larger structural components subjected to different loadings. Composite specimens should be treated as *structures* in themselves. Homogeneity at the continuum

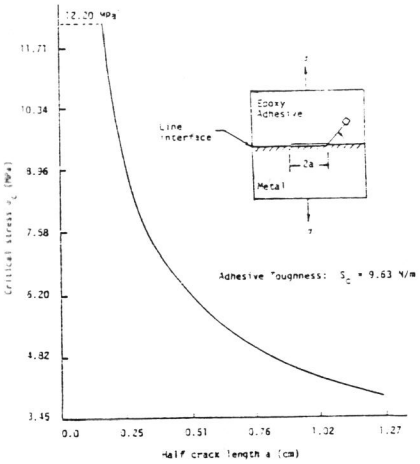

Fig. 8. Critical stress versus half crack length for preexisting crack at interface of adhesive and metal.

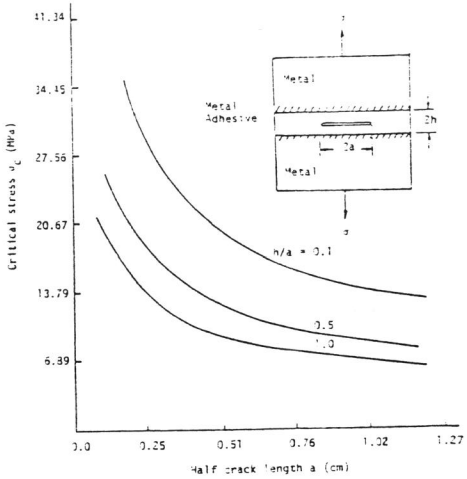

Fig. 9. Critical stress versus half crack length for precracked adhesive layer.

level applies only to the constituents; namely, the fiber and matrix material.

Defect Distribution

The general notion that defects or imperfections tend to weaken the strength of solids is obviously incorrect. Metals are known to contain many more defects than single crystals because of the presence of grain boundaries. Uniaxial tensile tests have shown, however, that the strength of aluminum alloys can reach 500 MPa or higher while the single crystal aluminum that contains no grain boundary may only have strength in the neighborhood of 10 MPa. The argument is that dislocations are then the cause of strength weakening in the single crystals. This explanation does not strictly hold because the strength of nearly pure aluminum becomes vanishingly small.

Strength, therefore, relies on the homogeneity arising from the combined *distribution* of load and defect. Under uniaxial tests, the variation or disorder among the grains in a metal is less than that among the dislocations in a single crystal. In a pure metal, the electron movements are even more chaotic or inhomogeneous. Strength must therefore be associated with the first order degree of homogeneity of the system tested at a predetermined energy input rate. Composite material specimens cannot satisfy the condition of homogeneity in metal testing and must therefore be treated accordingly.

Energy Density Fluctuation

The way with which energy is transferred from one unit volume of material to another changes for each increment of loading. Energy density distribution, say dW/dV, can be uniquely associated with material damage pattern at the

different scale levels depending on the size of the reference volume element. Figures 10(a) and 10(b) show the relative size of the volume element for a metal and composite compared with their internal structure. The nu-

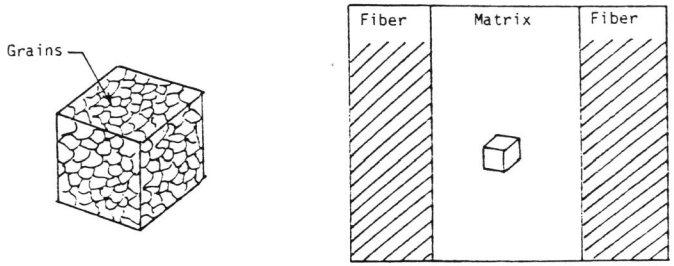

(a) Grains in a volume element (b) Volume element in matrix or fiber

Fig. 10. Reference volume element size compared to internal structure of metal and composite.

cleation and/or coalescence of pores in a single grain, the creation of microcracks in grains, and the separation of solids by macrocrack growth involve interaction of energy transfer with material microstructure. Loosely speaking, material microstructure becomes increasingly more important as energy transfer rate is lowered in the order of monotonically rising load, fatigue and creep. In engineering application, an assessment of local inhomogeneity with parameters than can be measured globally is essential.

As a rule, failure always initiates from the sites of material inhomogeneity and/or load concentration. The energy per unit volume, designated by dW/dV, will oscillate at these locations and possess relative maxima and minima. They are designated as $(dW/dV)_{max}$ and $(dW/dV)_{min}$ and have been shown by Sih (1973; 1981) to be related, respectively, to yielding initiation and fracture initiation. Of particular significance is the physical interpretation of the global and local stationary values of dW/dV given by the pair $[(dW/dV)^{max}_{max}]_{\ell}$, $[(dW/dV)^{max}_{max}]_{g}$ and $[(dW/dV)^{max}_{min}]_{\ell}$, $[(dW/dV)^{max}_{min}]_{g}$. The former is concerned with yielding and latter with fracture instability. In what follows, only $(dW/dV)_{min}$ will be discussed in connection with material inhomogeneity.

Interaction of Load and Material Inhomogeneity

The simple system of a single inclusion or foreign object with properties E_1, ν_1 embedded in a matrix possessing different properties E_2, ν_2 will be considered. The interaction of load type and material inhomogeneity will be demonstrated by subjecting the system to two different loading conditions and varying the ratio E_1/E_2. The Poisson's ratio ν_1 and ν_2 are taken to be equal. Figure 11 shows the composite system that has finite boundaries 2h × 2w. The uniform Load I has magnitude σ and the linearly decaying Load II vary as σ_o (1-x/w). The ends of the inclusion are shaped elliptically with semi-major and semi-minor axis a and b. The total length is denoted by 2c.

Stability of the nonhomogeneous system can be assessed through the length parameter "ℓ" that marks the distance between L and G in Fig. 11 such that they coincide, respectively, with the locations of $[(dW/dV)^{max}_{min}]_{\ell}$ and $[(dW/dV)^{max}_{min}]_{g}$. The points L and G always lie along the prospective path of failure. In general, there exists a multitude of local stationary values of dW/dV. In two-dimensions, they can be found by referring to a set of local coordinates, say at some point $p(x_j,y_j)$ (j = 1,2,...,n). The value of r_j can be fixed while stationary values of dW/dV are determined with reference to θ_j. Failure is assumed to initiate at the point of maximum $[(dW/dV)_{min}]_{\ell}$. The global stationary values of $[(dW/dV)_{min}]_{g}$ refer to a fixed coordinate system, say xy in Fig. 11, the maximum value of which $[(dW/dV)^{max}_{min}]_{g}$ determines the point G. This gives ℓ that serves as a measure of the combined influence of loading type and rate, specimen size and geometry, and material inhomogeneity on failure behavior of the overall system. For instance, the rate of loading may be decreased to reduce ℓ. This tends to localize failure that depends more on the material microstructure. A composite system can thus be divided into many subregions and only those which undergo active interaction with load and geometry require more detailed analysis. A rational means of quantitatively assessing material inhomogeneity can be developed.

Consider Loading I in Fig. 11. Numerical values of ℓ are found for σ = 689.5 MPa, E_2 = 68.95 GPa while E_1/E_2 is varied. With values of w = 15.88 cm, c = 12.70 cm, b/a = 0.5, three different ratios of h/w = 0.45, 0.50 and 0.55 are considered. Plotted in Fig. 12 are the results of ℓ versus E_1/E_2 (see also Table 5). The three solid lines are nearly straight except when they reach the upper limit ℓ = 3.18 cm corresponding to G on the boundary. For $E_1/E_2 < 1$, ℓ increases or decreases with E_1/E_2. The case of a notch is recovered in the limit as $E_1/E_2 \to 0$. Thus, reduction in E_1/E_2 and h/w result in more localized failure and enhances subcritical material damage. As $E_1/E_2 \to 1$, ℓ approaches the entire ligament w-c and failure tends to be more catastrophic as a greater portion of the solid is involved in the damage process at a given instant.

A linearly decaying load shown in Fig. 11 as Loading II is also analyzed. The maximum peak σ_o is 137.9 MPa and the other geometric parameters are the same as those for Loading I. Figure 13 reveals that ℓ does not increase as rapidly with E_1/E_2 as in the case of uniform loading. The failure behavior is therefore more stable. This is intuitively obvious because the ligament ahead of the inclusion experience a lower load magnitude. Table 6 gives the numerical values of ℓ for different E_1/E_2 ratios. Note that the values of ℓ in Table 6 are lower than those in Table 5. These two examples show that failure mode stability in a composite system depends sensitively on load type.

HEAT AND MOISTURE EFFECTS ON STRESSES IN COMPOSITES

High performance composite materials are now frequently used in aircraft and aerospace structures that encounter aggressive environments in service. Sudden change in surface moisture and/or temperature can permanently alter the

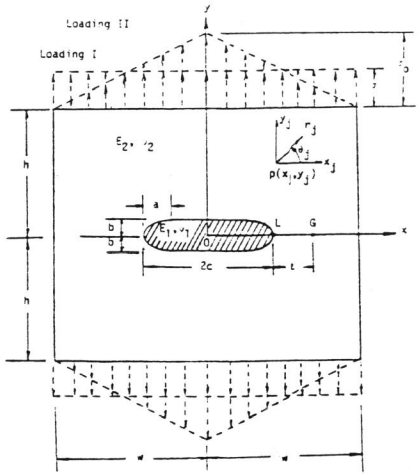

Fig. 11. An inhomogeneous system with finite dimensions subjected to mechanical loads.

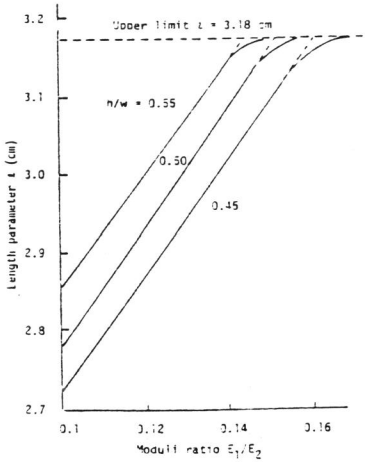

Fig. 12. Interaction of material inhomogeneity with uniformly applied load.

TABLE 5 Locations of Local and Global Stationary Values of Minimum Strain Energy Density Function for Uniform Loading

	ℓ (cm)		
E_1/E_2	h/w = 0.45	h/w = 0.50	h/w = 0.55
0.10	2.725	2.778	2.858
0.11	2.802	2.858	2.934
0.12	2.883	2.937	2.996
0.13	2.946	3.016	3.068
0.14	3.018	3.089	3.150
0.15	3.096	3.149	3.175
0.16	3.150	3.175	-
0.17	3.175	-	

mechanical stiffness and strength of composite laminates. These effects[14] lead to fluctuation of stresses and strains as a function of time and interact in a complex fashion with mechanical load, structural component geometry and composite type. Depending on the rapidity of the transient boundary conditions, heat, moisture and mechanical deformation can be coupled, an area that has received little or no attention until recently.

[14]The detrimental effect of stress corrosion in metals is now well-known.

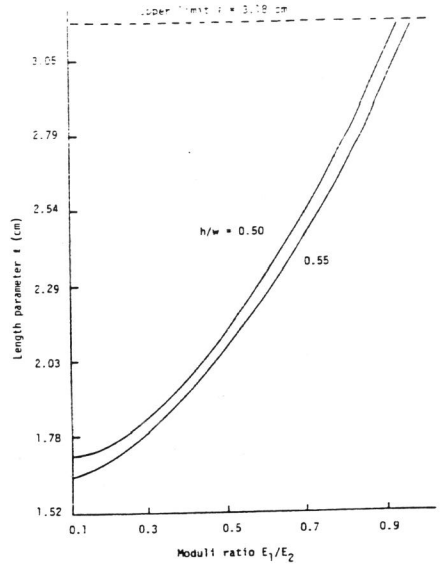

Fig. 13. Interaction of material inhomogeneity with a linearly decaying load.

TABLE 6 Locations of Local and Global Stationary Values of Minimum Strain Energy Density Function for Linearly Decaying Load

	ℓ (cm)	
E_1/E_2	h/w = 0.50	h/w = 0.55
0.1	1.640	1.693
0.2	1.693	1.746
0.3	1.799	1.826
0.4	1.985	1.958
0.5	2.064	2.117
0.6	2.249	2.302
0.7	2.434	2.514
0.8	2.646	2.725
0.9	2.910	2.995
0.95	3.043	3.149

Sih and Shih (1983) have derived a hygrothermal theory of elasticity that accounts for the interdependence of heat, moisture and mechanical deformation. The coupled governing equations for plane strain[15] are given by

[15]When diffusion and stress are coupled, the diffusion coefficients for plane strain must also be distinguished from those for plane stress as in the theory of plane elasticity.

$$D\nabla^2 C = \frac{\partial C}{\partial t} - \lambda \frac{\partial R}{\partial t}$$

$$\mathcal{D}\nabla^2 R = \frac{\partial R}{\partial t} - \nu \frac{\partial C}{\partial t} \tag{14}$$

in which C is the moisture concentration and R is associated with the temperature T and a stress function Ψ:

$$R = T + N\Psi \tag{15}$$

The function Ψ takes the form

$$\Psi = \sigma_{kk} + \frac{2E}{1-\nu_p}[\alpha(T-T_o) + \beta(C-C_o)] \tag{16}$$

with σ_{kk} being the first stress invariant. The thermal and moisture coefficients of expansion are denoted by α and β, respectively, while E and ν_p are the Young's modulus and Poisson's ratio. There are a total of five physical constants D, $\mathcal{D}$, λ, ν and N in this theory.

Physical Constants

One of the main reasons why coupled theories of heat, moisture and stress have not advanced is due to the lack of a knowledge of the physical constants. Sih, Shih and Chou (1980) have devised a method for extracting the coupling constants by matching the coupled solution with the experimental results on T300/5208 graphite epoxy for composite laminates. The values for plane strain derived by Sih and Shih (1983) will be used:

$$D = 2.440 \times 10^{-6}\ cm^2/hr,\ \lambda = 0.0445\ Kg/°Cm^3$$

$$\mathcal{D} = 1.186 \times 10^{-5}\ cm^2/hr,\ \nu = 1.3439\ °Cm^3/Kg \tag{17}$$

$$N = 1.1240 \times 10^{-8}\ °Cms^2/Kg$$

The remaining constants α, β, ν_p and E are

$$\alpha = 4.154 \times 10^{-5}/°C,\ \nu_p = 0.493$$

$$\beta = 3.591 \times 10^{-3}/wt\%H_2O,\ E = 75.933\ GPa \tag{18}$$

Without going into details, only the variation of stress intensity factor k_1 with the time parameter $D_t t/d^2$ will be discussed where d is the specimen thickness and D_t is a time scale factor chosen to be 1.0 cm^2/hr.

Sudden Temperature Rise

Referring to Fig. 14, the surface temperature on an elliptically-shaped crack Γ_1 with major and minor axis 2a and 2b is raised suddenly from 21°C to 61°C. The relative humidity is kept constant at 75% RH. The conditions

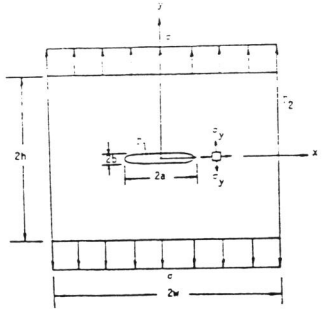

Fig. 14. Elliptical-like crack in a T300/5208 graphite/epoxy composite panel.

on the outer boundary Γ_2 with h = 3 cm and w = 4 cm is maintained constant at 75% RH and 21°C for all time. Four different applied stress levels will be considered. They involve tension and compression with σ = ±50 MPa and ±100 MPa. The sharpness of the crack measured by a/b is fixed at the ratio 10:1.

Chou, Sih and Shih (1984) have obtained results for the stress intensity factor

$$k_1 = \frac{1}{2}\sigma_m\sqrt{\rho} = \sigma\sqrt{a}\left[1 + \frac{1}{2}\frac{\sigma_t}{\sigma}\sqrt{\frac{a}{\rho}}\right] \tag{19}$$

where σ_m is the local normal stress acting in the element shown in Fig. 14 and ρ is the crack tip radius of curvature. The stress σ_t may be positive or negative depending on the instantaneous combined influence of temperature and moisture diffusion. Positive σ applies to tensile mechanical loading and negative σ to compressive mechanical loading. A plot of $k_1/\sigma\sqrt{a}$ versus $D_t t/d^2$ is shown in Fig. 15 for tensile loading of σ = 50 and 100 MPa. Uncoupling refers only to noninvolvement of mechanical deformation. Temperature and moisture diffusion are always coupled in this discussion. The transient character of the solution is more pronounced at σ = 50 MPa where k_1 is seen to increase with time and then gradually approaches a limit. The time dependency is overshadowed by the applied mechanical stress when σ is raised to 100 MPa in which case the curves are almost flat. Stress uncoupling tends to yield conservative results for sudden temperature rise on the crack as the dotted curves are higher than the solid ones in Fig. 15. The situation is reversed in Fig. 16 if compressive mechanical stress is applied with σ = -50 and -100 MPa.

Even though the differences between the coupled and uncoupled results are moderate in the examples cited, they cannot be ignored in general. Sih and Shih (1983) and Chou, Sih and Shih (1984) have shown in other instances where coupling can significantly alter the results, both quantitatively and qualitatively. The difference depends on load type, geometry and material inhomogeneity.

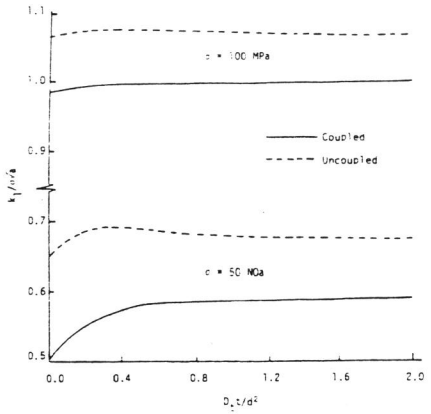

Fig. 15. Stress intensity factor versus time as temperature on crack changes from 21°C to 61°C for 75% RH with a/b = 10 and tensile loading.

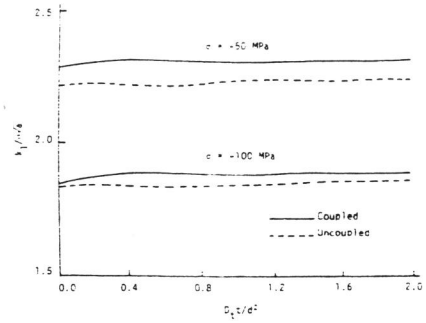

Fig. 16. Stress intensity factor versus time as temperature on crack changes from 21°C to 61°C for 75% RH with a/b = 10 and compressive loading.

CONCLUDING REMARKS

Composites are multicomponent materials and nonhomogeneous. Their behavior is complex because of the additional inhomogeneity introduced by defects that are created during manufacturing and can grow with load. Characterizing composite specimen behavior under simple loading, therefore, serves little purpose in terms of gaining useful design information unless the data can be used to predict situations other than those tested. Local energy dissipation, depending on the rate of energy transfer in a unit volume of material, can be used to identify failure mode. It is well-known experimentally that loading rate alone can control material behavior changing from elastic to elastic-plastic, viscoelastic or viscoplastic without altering the metallurgical or physical properties of the material. Permanent material damage associated with defects at the different scale level must be accounted for.

The establishment of threshold values of the strain energy density function with different material damage modes is a concept that can be consistently applied to explain the variety of composite material behavior. With the advent of modern computers, the rate of material damage can be treated incrementally simply by nonlinear stress and failure analysis in tandem such that damage is accumulated for each increment of loading. The constitutive relation for each material element can be derived accordingly without making an a priori assumption as it is now done in the classical continuum theory approach. Accumulative damage concept has already been incorporated into the strain energy density theory and applied successfully to explain the behavior of metal with strain hardening (Sih and Matic, 1982) and concrete with bilinear softening (Carpinteri and Sih, 1984). Application of the dW/dV concept to composite systems is case specific because material damage is strictly a load time history dependent process.

REFERENCES

Fracture of Composite Materials, (1979). Edited by G. C. Sih and V. P. Tamuzs, Sijthoff and Noordhoff Publishers, Alphen aan den Rijn.

Fracture of Composite Materials, (1981). Edited by G. C. Sih and V. P. Tamuzs, Martinus Nijhoff Publishers, The Hague.

Sih, G. C. (1976). Fracture toughness concept, American Society of Testing Materials, ASTM STP 605, pp. 3-15.

Sih, G. C., Hilton, P. D., Badaliance, R., Shenberger, P. S. and Villarreal, G. (1973). Fracture mechanics of fibrous composites, American Society of Testing Materials, ASTM STP 521, pp. 98-132.

Wu, E. M. and Reuter, R. C. (1965). Crack extension in fiber-glass reinforced plastics, University of Illinois TAM Report No. 275.

Lauraitis, K. (1971). Tensile strength of off-axis unidirectional composites, University of Illinois TAM Report No. 344.

Lauraitis, K. (1971). Failure modes and strength of angle-ply laminates, University of Illinois TAM Report No. 345.

Sih, G. C., Chen, E. P., Huang, S. L. and McQuillen, E. J. (1975). Material characterization on the fracture of filament-reinforced composites, J. of Composite Materials, Vol. 9, pp. 167-186.

Sih, G. C. and Chen, E. P. (1973). Fracture analysis of unidirectional composites, J. of Composite Materials, Vol. 7, pp. 230-244.

Hilton, P. D. and Sih, G. C. (1972). A sandwiched layer of dissimilar material weakened by crack-like imperfections, Proceedings of the 5th Southeastern Conference on Theoretical and Applied Mechanics, Vol. 5, pp. 123-149.

Sih, G. C. (1973). A special theory of crack propagation, in Mechanics of Fracture, Vol. I: Methods of Analysis and Solutions of Crack Problems, edited by G. C. Sih, Noordhoff International Publishing, The Netherlands, pp. 21-45.

Sih, G. C. (1981). Experimental fracture mechanics: strain energy density criterion, Experimental Evaluation of Stress Concentration and Intensity Factors, edited by G. C. Sih, Martinus Nijhoff Publishers, The Hague, pp. XVII-LVI.

Sih, G. C. and Chen, E. P. (1981). Cracks in Composite Materials, Martinus Nijhoff Publishers, The Hague.

Plane Strain Crack Toughness Testing of High Strength Metallic Materials, (1966). Edited by W. F. Brown, Jr. and J. E. Srawley, American Society of Testing Materials, ASTM STP 410.

Sih, G. C. and Chen, E. P. (1973). Fracture analysis of unidirectional and angle-ply composites, Technical Report NADC-TR-73-1, IFSM 73-26, Institute of Fracture and Solid Mechanics, Lehigh University.

Sih, G. C. and Moyer, E. T., Jr. (1979). Influence of interface in composite failure, Advanced Composites, Proceedings of Conference on Advanced Composites, Technology Conferences, El Segundo, California.

Rice, J. R. and Sih, G. C. (1965). Plane problems of cracks in dissimilar materials, J. of Applied Mechanics, Vol. 32, pp. 418-423.

Sih, G. C. (1973). Handbook of Stress Intensity Factors, Institute of Fracture and Solid Mechanics, Lehigh University Publication, Bethlehem, Pa.

Sih, G. C. (1984, in press). The state of affairs near the crack tip, Proceedings on Modelling Problems in Crack Tip Mechanics, edited by J. T. Pindera, Martinus Nijhoff Publishers, The Netherlands.

Sih, G. C. and Shih, M. T. (1983). A generalized coupled theory of hygrothermal-elasticity: transient effects in composite laminate with circular cavity, AMMRC TR 83-56.

Sih, G. C., Shih, M. T. and Chou, S. C. (1980). Transient hygrothermal stresses in composites: coupling of moisture and heat with temperature varying diffusivity, Int. J. Engng. Sci., Vol. 18, pp. 19-42.

Chou, S. C., Sih, G. C. and Shih, M. T. (1984). Moisture and temperature effects on the transient stresses around crack-like defects, presented at International Conference on Application of Fracture Mechanics to Materials and Structures, Freiburg, Germany.

Sih, G. C. and Matic, P. (1982). A pseudo-linear analysis of yielding and crack growth: strain energy density criterion, Proceedings on Defects, Fracture and Fatigue, edited by G. C. Sih and J. W. Provan, Martinus and Nijhoff Publishers, The Hague, pp. 223-232.

Carpinteri, A. and Sih, G. C. (1984). Damage accumulation of crack growth in bilinear materials with softening: strain energy density theory, J. of Theoretical and Applied Fracture Mechanics, Vol. 1, No. 2.